

Supporting Information

Prediction of Structural Stability and Explosive Performance of N-rich Mo-N Compounds under High Pressures

Jianyan Lin, Xin Liu, and Guangmin Yang*

College of Physics, Changchun Normal University, Changchun 130032, China

*Address correspondence to: yangguangmin@mail.ccsfu.edu.cn

Index	Page
1. Computational details	2
2. Phonon dispersion curves for the predicted Mo-N compounds	4
3. Crystal structures of <i>P4/mnc</i> MoN ₈ and <i>Immm</i> MoN ₈ at 1 atm	5
4. Electronic band structures of the predicted Mo-N compounds	5
5. Explosive performance of <i>P6₃/mmc</i> MoN ₂ , <i>P4/mbm</i> MoN ₂ , <i>Immm</i> MoN ₈	6
6. Comparison of detonation parameters by various methods	6
7. Elastic constants of the predicted Mo-N compounds at 1 atm	7
8. Structural information of the predicted stable compounds	9
9. References	11

Computational Details

Our structural prediction approach is based on a global minimization of free energy surfaces merging *ab initio* total-energy calculations with CALYPSO (Crystal structure AnaLYsis by Particle Swarm Optimization) methodology as implemented in the CALYPSO code.^{1,2} The structures of stoichiometry Mo_xN_y ($x = 1, y = 1 - 11$; $x = 2, y = 1, 3$; $x = 3, y = 1, 2, 4, 5$; $x = 4, y = 1, 3, 5$; $x = 5, y = 1, 4, 6$) were searched with simulation cell sizes of 1 - 4 formula units (f.u.) at 1 atm and 25, 50, 100, 200 GPa. In the first step, random structures with certain symmetry are constructed in which atomic coordinates are generated by the crystallographic symmetry operations. Local optimizations using the VASP code³ were done with the conjugate gradients method and stopped when total energy changes became smaller than 1×10^{-5} eV per cell. After processing the first generation structures, 60% of them with lower enthalpies are selected to construct the next generation structures by PSO (Particle Swarm Optimization). 40% of the structures in the new generation are randomly generated. A structure fingerprinting technique of bond characterization matrix is applied to the generated structures, so that identical structures are strictly forbidden. These procedures significantly enhance the diversity of the structures, which is crucial for structural global search efficiency. In most cases, structural searching simulations for each calculation were stopped after generating 1000 ~ 1200 structures (e.g., about 20 ~ 30 generations).

Structural optimization and electronic structure calculations were performed with the framework of density functional theory (DFT)^{4,5} within the Perdew-Burke-Ernzerhof (PBE)⁶ functional of the generalized gradient approximation (GGA),⁷ as implemented by the VASP (Vienna *Ab initio* Simulation Package) code. The all-electron projector augmented-wave (PAW)⁸ pseudopotentials of Mo and N treat $4d^55s^1$ and $2s^22p^3$ electrons as the valence electrons, respectively. The cutoff energy was set at 700 eV, and Monkhorst-Pack scheme⁹ with a k -point grid of $2\pi \times 0.03 \text{ \AA}^{-1}$ in Brillouin zone was selected to ensure that all enthalpy calculations converged to less than 1 meV per atom. The dynamical stability of predicted structures was

determined by phonon calculations using a supercell approach with the finite displacement method¹⁰ as implemented in the Phonopy code.¹¹ Crystal orbital Hamilton population (COHP) analysis giving the information on the interatomic interaction was implemented in the LOBSTER package.^{12,13} The calculation accuracy is consistent with that of the other parts. The electron localization function (ELF)¹⁴ was calculated using VASP code.

Supplementary Figures

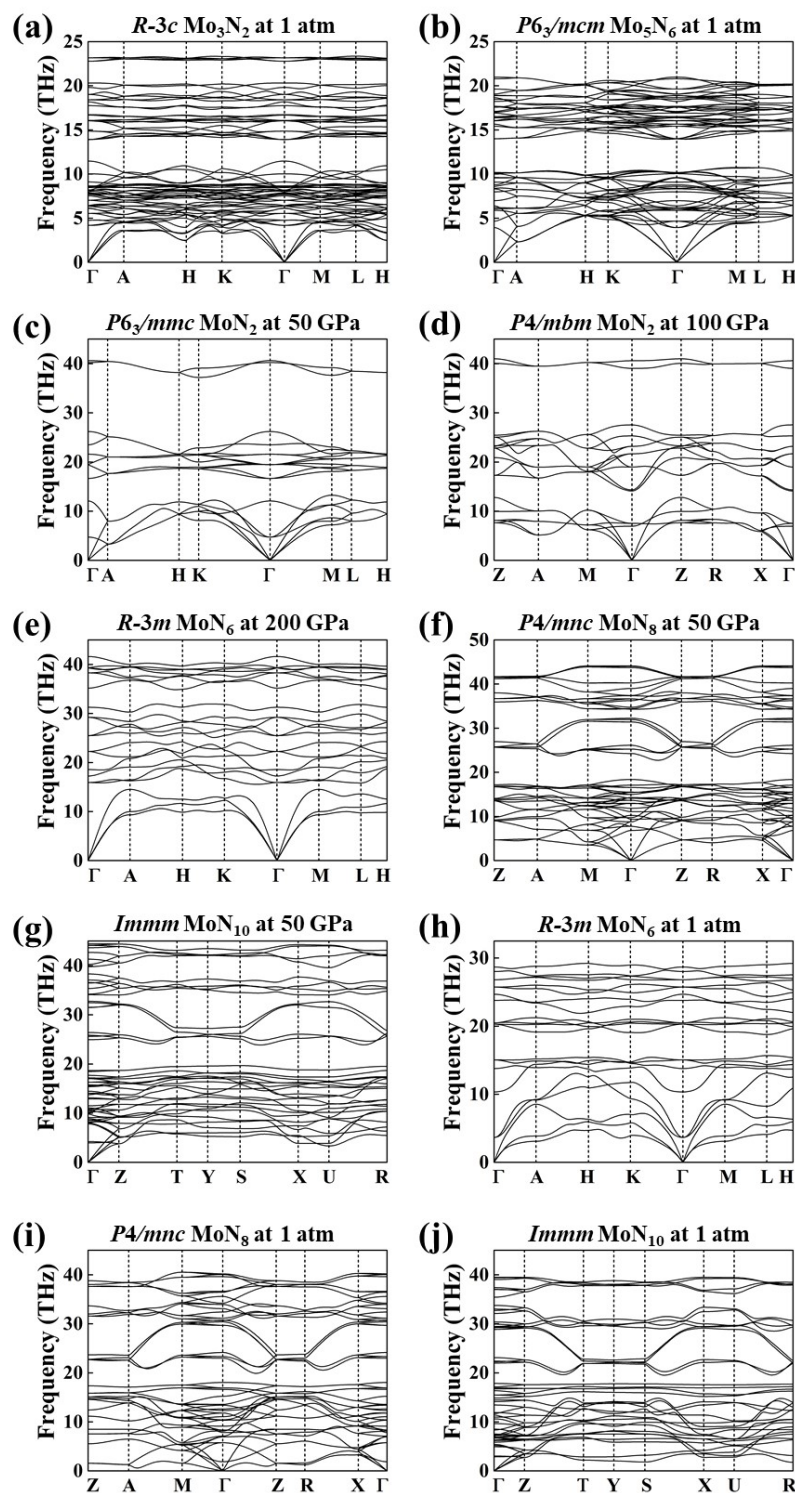


Figure S1. Phonon dispersion curves of the predicted Mo-N binary compounds. The absence of any imaginary frequency modes in the first Brillouin zone indicates the dynamical stability of the predicted compounds.

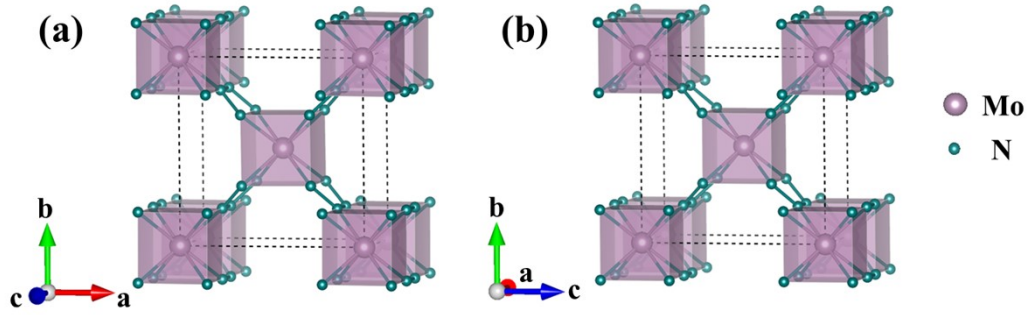


Figure S2. Crystal structures of (a) MoN_8 in $P4/mnc$ symmetry at 1 atm, (b) MoN_8 in $Immm$ symmetry after the removal of isolated N_2 of $Immm$ MoN_{10} at 1 atm.

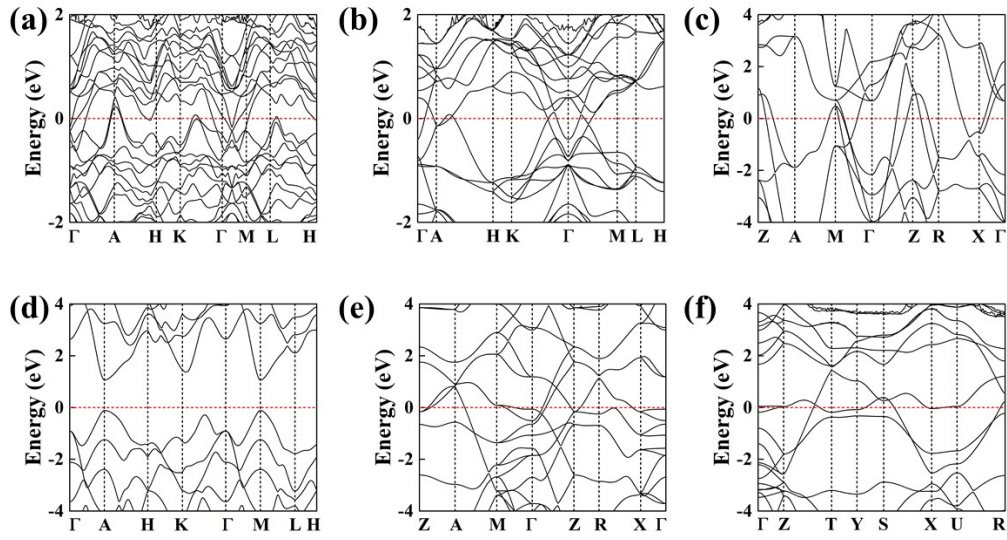


Figure S3. Electronic band structures for (a) $R-3c$ Mo_3N_2 at 1 atm, (b) $P6_3/mcm$ Mo_5N_6 at 1 atm, (c) $P4/mbm$ MoN_2 at 100 GPa, (d) $R-3m$ MoN_6 at 200 GPa, (e) $P4/mnc$ MoN_8 at 50 GPa and (f) $Immm$ MoN_{10} at 50 GPa.

Supplementary Table

Table S1. Calculated mass density (ρ), energy density (E_d), volumetric energy density (E_v), detonation velocity (V_d), and detonation pressure (P_d) of the predicted $P6_3/mmc$ MoN_2 , $P4/mbm$ MoN_2 , and $Immm$ MoN_8 , compared with TNT, and HMX.

Compounds	ρ (g cm ⁻³)	E_d (kJ g ⁻¹)	E_v (kJ cm ⁻³)	V_d (km s ⁻¹)	P_d (GPa)
<i>P6₃/mmc</i> MoN_2	7.15	0.07	0.50	2.74	5.52
<i>P4/mbm</i> MoN_2	7.93	1.04	8.25	5.93	26.40
<i>Immm</i> MoN_8	3.84	2.51	9.64	8.81	48.66
TNT ¹⁵	1.64	4.30	7.05	6.90	19.00
HMX ¹⁵	1.90	5.70	10.83	9.10	39.30

The following decomposition reactions are considered to determine the energy density and detonation parameters:

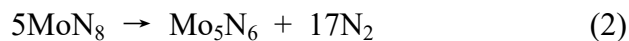


Table S2. Comparison of detonation velocity (V_d), and detonation pressure (P_d) calculated by different methods of the predicted compounds.

Compounds	V_d (km s ⁻¹)			P_d (GPa)	
	<i>K-J</i> ¹⁶	<i>W</i> ¹⁷	<i>Stine-S2</i> ¹⁸	<i>K-J</i> ¹⁶	<i>W</i> ¹⁷
<i>R-3m</i> MoN_6	18.25	12.41	20.57	251.61	210.56
<i>P4/mnc</i> MoN_8	11.71	9.75	13.69	94.69	87.06
<i>Immm</i> MoN_{10}	12.16	10.34	14.03	100.21	91.62
<i>Immm</i> MoN_8	8.81	7.46	10.86	48.66	38.23
<i>P6₃/mmc</i> MoN_2	2.74	2.41	8.13	5.52	6.93
<i>P4/mbm</i> MoN_2	5.93	3.43	9.88	26.40	15.56

Table S3. The calculated elastic constants C_{ij} in GPa for the predicted compounds.

	<i>P4/mbm</i> MoN ₂	<i>R-3m</i> MoN ₆	<i>P4/mnc</i> MoN ₈	<i>Immm</i> MoN ₁₀
C_{11}	685.411	567.519	215.028	750.032
C_{22}	685.411	567.519	215.028	233.050
C_{33}	735.730	640.244	784.565	262.655
C_{44}	235.246	315.758	120.632	122.910
C_{55}	235.246	315.758	120.632	95.7957
C_{66}	244.584	242.287	109.752	98.4681
C_{12}	184.014	82.9454	176.725	19.7664
C_{13}	162.492	111.652	47.5058	16.3849
C_{23}	162.492	111.652	47.5058	112.869
C_{14}		-45.4841		
C_{24}		45.4841		
C_{56}		-45.4841		

For *P4/mbm* MoN₂ and *P4/mnc* MoN₈ with tetragonal symmetry, the mechanical stability can be judged from the following criterion:

$$C_{11} > |C_{12}|,$$

$$2C_{13}^2 < C_{33}(C_{11} + C_{12}),$$

$$C_{44} > 0, C_{66} > 0.$$

For *R-3m* MoN₆ with rhombohedral symmetry, the mechanical stability can be judged from the following criterion:

$$C_{11} > |C_{12}|, C_{44} > 0,$$

$$C_{13}^2 < \frac{1}{2}C_{33}(C_{11} + C_{12}),$$

$$C_{14}^2 < \frac{1}{2}C_{44}(C_{11}-C_{12}) \equiv C_{44}C_{66}.$$

For *Immm* MoN₁₀ with orthohombic symmetry, its mechanical stability can be judged from the following criterion:

$$C_{11} > 0, C_{11}C_{22} > C_{12}^2,$$

$$C_{11}C_{22}C_{33} + 2C_{12}C_{13}C_{23} - C_{11}C_{23}^2 - C_{22}C_{13}^2 - C_{33}C_{12}^2 > 0,$$

$$C_{44} > 0, C_{55} > 0, C_{66} > 0$$

Table S4. Structural parameters of the predicted stable compounds.

Phases	Pressure (GPa)	Lattice Parameters (Å,°)	Wyckoff Positions (fractional)			
			Atoms	<i>x</i>	<i>y</i>	<i>z</i>
<i>R-3c</i> Mo ₃ N ₂	0	<i>a</i> = 10.23790	Mo(12f)	-0.88698	-0.18582	-0.53631
		<i>b</i> = 10.23790	N(2b)	0.00000	0.00000	0.00000
		<i>c</i> = 10.23790	N(6e)	-0.41626	-0.75000	-0.08374
		α = 28.2871				
		β = 28.2871				
		γ = 28.2871				
<i>P6₃/mcm</i> Mo ₅ N ₆	0	<i>a</i> = 4.90240	Mo(4d)	0.33333	0.66667	0.50000
		<i>b</i> = 4.90240	Mo(4c)	0.33333	0.66667	0.25000
		<i>c</i> = 11.16220	Mo(2a)	0.00000	0.00000	0.25000
		α = 90.0000	N(12k)	0.33829	-0.00000	0.63011
		β = 90.0000				
		γ = 120.0000				
<i>P6₃/mmc</i> MoN ₂	50	<i>a</i> = 2.78490	Mo(2c)	0.33333	0.66667	0.25000
		<i>b</i> = 2.78490	N(4e)	0.00000	0.00000	0.41262
		<i>c</i> = 7.62090				
		α = 90.0000				
		β = 90.0000				
		γ = 120.0000				
<i>P4/mbm</i> MoN ₂	100	<i>a</i> = 4.07760	Mo(2b)	-0.00000	0.00000	0.50000
		<i>b</i> = 4.07760	N(4g)	0.61486	0.88514	0.00000
		<i>c</i> = 2.59600				
		α = 90.0000				
		β = 90.0000				
		γ = 90.0000				
<i>R-3m</i> MoN ₆	200	<i>a</i> = 5.54900	Mo(3a)	0.00000	0.00000	0.00000
		<i>b</i> = 5.54900	N(18h)	0.12357	0.24713	-0.41955
		<i>c</i> = 4.09600				
		α = 90.0000				
		β = 90.0000				
		γ = 120.0000				
<i>P4/mnc</i> MoN ₈	50	<i>a</i> = 5.97570	Mo(2b)	0.00000	0.00000	0.50000

		$b = 5.97570$	N(16i)	0.57838	0.77806	1.31992
		$c = 3.61150$				
		$\alpha = 90.0000$				
		$\beta = 90.0000$				
		$\gamma = 90.0000$				
<i>Immm</i> MoN₁₀	50	$a = 3.59590$	Mo(2c)	0.00000	0.00000	0.50000
		$b = 6.46790$	N(16o)	0.82066	0.68841	0.18183
		$c = 6.78660$	N(4e)	0.65490	0.00000	0.00000
		$\alpha = 90.00000$				
		$\beta = 90.00000$				
		$\gamma = 90.00000$				

References

- (1) Wang, Y.; Lv, J.; Zhu, L.; Ma, Y. Crystal structure prediction via particle-swarm optimization. *Phys. Rev. B* **2010**, *82*, 094116.
- (2) Wang, Y.; Lv, J.; Zhu, L.; Ma, Y. CALYPSO: A method for crystal structure prediction. *Comput. Phys. Commun.* **2012**, *183*, 2063-2070.
- (3) Kresse, G.; Furthmüller, J. Efficient iterative schemes for ab initio total-energy calculations using a plane-wave basis set. *Phys. Rev. B* **1996**, *54*, 11169-11186.
- (4) Hohenberg, P.; Kohn, W. Inhomogeneous Electron Gas. *Phys. Rev.* **1964**, *136*, B864-B871.
- (5) Kohn, W.; Sham, L. J. Self-Consistent Equations Including Exchange and Correlation Effects. *Phys. Rev.* **1965**, *140*, A1133-A1138.
- (6) Perdew, J. P.; Burke, K.; Ernzerhof, M. Generalized Gradient Approximation Made Simple. *Phys. Rev. Lett.* **1996**, *77*, 3865-3868.
- (7) Perdew, J. P.; Chevary, J. A.; Vosko, S. H.; Jackson, K. A.; Pederson, M. R.; Singh, D. J.; Fiolhais, C. Atoms, molecules, solids, and surfaces: Applications of the generalized gradient approximation for exchange and correlation. *Phys. Rev. B* **1992**, *46*, 6671-6687.
- (8) Blöchl, P. E. Projector augmented-wave method. *Phys. Rev. B* **1994**, *50*, 17953-17979.
- (9) Monkhorst, H. J.; Pack, J. D. Special points for Brillouin-zone integrations. *Phys. Rev. B* **1976**, *13*, 5188-5192.
- (10) Parlinski, K.; Li, Z. Q.; Kawazoe, Y. First-Principles Determination of the Soft Mode in Cubic ZrO₂. *Phys. Rev. Lett.* **1997**, *78*, 4063-4066.
- (11) Togo, A.; Oba, F.; Tanaka, I. First-principles calculations of the ferroelastic transition between rutile-type and CaCl₂-type SiO₂ at high pressures. *Phys. Rev. B* **2008**, *78*, 134106.
- (12) Dronskowski, R.; Blochl, P. E. Crystal orbital Hamilton populations (COHP): energy-resolved visualization of chemical bonding in solids based on density-functional calculations. *J. Phys. Chem.* **1993**, *97*, 8617-8624.

- (13) Maintz, S.; Deringer, V. L.; Tchougréeff, A. L.; Dronskowski, R. LOBSTER: A tool to extract chemical bonding from plane-wave based DFT. *J. Comput. Chem.* **2016**, *37*, 1030-1035.
- (14) Becke, A. D.; Edgecombe, K. E. A simple measure of electron localization in atomic and molecular systems. *J. Chem. Phys.* **1990**, *92*, 5397-5403.
- (15) Kamlet, M. J.; Dickinson, C. Chemistry of detonations. III. Evaluation of the simplified calculational method for chapman - jouguet detonation pressures on the basis of available experimental information, *J. Chem. Phys.* **1968**, *48*, 43-50.
- (16) Kamlet, M. J.; Jacobs, S. J. Chemistry of detonations. I. A simple method for calculating detonation properties of C-H-N-O explosives, *J. Chem. Phys.* **1968**, *48*, 23-35.
- (17) Wu, X. A simple method for calculating detonation parameters of explosives, *J. Energ. Mater.* **1985**, *3*, 263-277.
- (18) Stine, J. R. On predicting properties of explosives – detonation velocity, *J. Energ. Mater.* **1990**, *8*, 41-73.
- (19) Mouhat F, Coudert F-X. Necessary and sufficient elastic stability conditions in various crystal systems, *J. Phys Rev B.* **2014**, *90*(22): 224104.